



# Preoperative Breast Magnetic Resonance Imaging as a Predictor of Response to Neoadjuvant Chemotherapy

Robert Browne<sup>1</sup> , Peter McAnena<sup>1</sup>, Niamh O'Halloran<sup>2</sup>, Brian M Moloney<sup>2</sup>, Emily Crilly<sup>1</sup>, Michael J Kerin<sup>1,3</sup> and Aoife J Lowery<sup>1,3</sup>

<sup>1</sup>Department of Surgery, University Hospital Galway, Galway, Ireland. <sup>2</sup>Department of Radiology, University Hospital Galway, Galway, Ireland. <sup>3</sup>Discipline of Surgery, Lambe Institute for Translational Research, National University of Ireland Galway, Galway, Ireland.

Breast Cancer: Basic and Clinical Research  
Volume 16: 1–11  
© The Author(s) 2022  
Article reuse guidelines:  
sagepub.com/journals-permissions  
DOI: 10.1177/11782234221103504  


## ABSTRACT

**INTRODUCTION:** The ability to accurately predict pathologic complete response (pCR) after neoadjuvant chemotherapy (NAC) in breast cancer would improve patient selection for specific treatment strategies, would provide important information for patients to aid in the treatment selection process, and could potentially avoid the need for more extensive surgery. The diagnostic performance of magnetic resonance imaging (MRI) in predicting pCR has previously been studied, with mixed results. Magnetic resonance imaging performance may also be influenced by tumour and patient factors.

**METHODS:** Eighty-seven breast cancer patients who underwent NAC were studied. Pre-NAC and post-NAC MRI findings were compared with pathologic findings postsurgical excision. The impact of patient and tumour characteristics on MRI accuracy was evaluated.

**RESULTS:** The mean (SD) age of participants was 48.7 (10.3) years. The rate of pCR based on post-NAC MRI was 19.5% overall (19/87). The sensitivity, specificity, positive predictive value (PPV), negative predictive value, and accuracy in predicting pCR were 52.9%, 77.1%, 36.0%, 87.1%, and 72.4%, respectively. Positive predictive value was the highest in nonluminal versus Luminal A disease (45.0% vs 25.0%,  $P < .001$ ), with higher rates of false positivity in nonluminal subtypes ( $P = .002$ ). Tumour grade, T category, and histological subtype were all independent predictors of MRI accuracy regarding post-NAC tumour size.

**CONCLUSION:** Magnetic resonance imaging alone is insufficient to accurately predict pCR in breast cancer patients post-NAC. Magnetic resonance imaging predictions of pCR are more accurate in nonluminal subtypes. Tumour grade, T category, and histological subtype should be considered when evaluating post-NAC tumour sizes.

**KEYWORDS:** Breast cancer, neoadjuvant chemotherapy, MRI, grade, pathology

**RECEIVED:** January 15, 2022. **ACCEPTED:** April 28, 2022.

**TYPE:** Original Research

**FUNDING:** The author(s) received no financial support for the research, authorship, and/or publication of this article.

**DECLARATION OF CONFLICTING INTERESTS:** The author declared no potential conflicts of interest with respect to the research, authorship, and/or publication of this article.

**CORRESPONDING AUTHOR:** Robert Browne, Department of Surgery, University Hospital Galway, Galway, Ireland. Email: robertebrowne@gmail.com

## Introduction

Breast cancer is the most common female cancer and the second most common cause of female cancer death, with an increasing incidence worldwide.<sup>1</sup> The modern paradigm of breast cancer management involves a combination of surgery, radiotherapy, chemotherapy, and targeted therapies, depending on the tumour phenotype and disease stage at presentation.<sup>2</sup> The evidence for the safety and efficacy of neoadjuvant (pre-surgery) chemotherapy (NAC) continues to grow, and this approach can be very useful, when indicated.<sup>3</sup>

Neoadjuvant chemotherapy can convey a number of benefits to the patient including reducing the size of the tumour and potentially the disease stage, allowing less-invasive surgery to be performed.<sup>4</sup> The use of NAC has allowed the modern breast surgeon to opt for a breast-conserving approach, in combination with sentinel lymph node biopsy, where once a mastectomy with axillary dissection would have been indicated in selected cases.<sup>5</sup> Neoadjuvant chemotherapy has become the standard of care for inflammatory and locally advanced breast cancers, and its use is increasing in breast cancers overexpressing the human

epidermal growth factor 2 (HER2), in triple-negative breast cancers, where it offers the opportunity to monitor the tumour response to systemic therapy in vivo and provides valuable information relating to long-term prognosis.

An additional potential benefit of NAC in breast cancer may be obviating the need for surgery by achieving a complete response/complete tumour regression in the breast through systemic therapy alone.<sup>6</sup> The absence of residual tumour in the surgically resected specimen post-NAC is termed a pathologic complete response (pCR). Achieving pCR has been associated with favourable outcomes and is generally used as a surrogate endpoint in evaluating response to therapy.<sup>7,8</sup>

Magnetic resonance imaging (MRI) is the modality that has shown most promise in predicting pCR in breast cancer. The accuracy of MRI exceeds that of mammography and physical examination in predicting pathologic tumour size in patients post-NAC, although preliminary studies investigating nuclear medicine imaging have demonstrated a potential role.<sup>9–11</sup> The rates of pCR post-NAC vary widely in the literature (between 0.3% and 50.3%), and reports of MRI accuracy in



Creative Commons Non Commercial CC BY-NC: This article is distributed under the terms of the Creative Commons Attribution-NonCommercial 4.0 License (<https://creativecommons.org/licenses/by-nc/4.0/>) which permits non-commercial use, reproduction and distribution of the work without further permission provided the original work is attributed as specified on the SAGE and Open Access pages (<https://us.sagepub.com/en-us/nam/open-access-at-sage>).

predicting pCR are similarly varied.<sup>12</sup> Magnetic resonance imaging accuracy has also been shown to vary according to molecular subtype, with MRI being least accurate for Luminal A and some Luminal B subtype tumours, which also have the lowest rates of pCR.<sup>13,14</sup>

The primary aim of this study was to assess the ability of MRI to accurately predict pCR in breast cancer patients post-NAC, investigating how often a radiologic complete response (rCR) corresponds to pCR in a cohort of patients who received NAC followed by surgery. The secondary aim is to investigate factors influencing the accuracy of MRI in predicting pathologic tumour size.

## Methods

### *Clinical database*

This monocentric, retrospective observational cohort study was undertaken at Galway University Hospital (GUH), a tertiary referral specialist breast cancer unit. This study received ethical approval from the Research Ethics Committee at GUH. All breast cancer patients between January 2007 and January 2015 who received NAC and had pre-NAC and post-NAC MRI scans performed were selected for this study. Selection was from a prospectively maintained institutional database including patient demographics, tumour pathology, and medical and surgical therapeutic information. Discussions and consensus at multidisciplinary team meetings including medical oncology, surgery, radiology, and radiation oncology were used to make clinical decisions relating to therapy in these patients. Patients who underwent combined neoadjuvant chemoradiotherapy – with no clear mass lesion visible on pre-NAC MRI and with multicentric, inflammatory, and/or metastatic disease at presentation – were excluded from this study.

### *MRI protocol*

Contrast-enhanced MRI analyses were performed on a short bore 1.5T magnet (Magnetom Espree 1.5T, Siemens Healthineers, Erlangen, Germany). Eight-channel breast phase array breast coil was used for signal reception. The following protocol was employed: sagittal T2 (repetition time (TR)/echo time (TE)=6570/111, gap=1 mm, flip angle=160°, matrix=340×75), axial T2 FS fl3d precontrast (TR/TE=5.15/2.39, gap=0.6 mm, flip angle=10°, matrix=320×100), and sagittal T1 fl3d (TR/TE=5.18/1.64, gap=0.6 mm, flip angle=10°, matrix=320×100). Dynamic axial T1 FS fl3d imaging was completed 5 times following the administration of contrast, with contrast material administered at a maximum dose of 0.1 mmol kg<sup>-1</sup> of body weight and with peak enhancement within the first 2 minutes. Contrast injection was performed using a power injector at a flow rate of 2 mL seconds<sup>-1</sup>, with contrast material flushed with a 20-mL physiological saline flush. Primary contrast-enhanced imaging was acquired at 90 seconds postcontrast administration, with

subsequent imaging acquired acquisitions within 5 to 7 minutes.<sup>1</sup> The section thickness was 3 mm for all sequences. The contrast employed was Gadoterate meglumine (Gd-DOTA).<sup>15</sup> Tumour size was calculated by measuring (in mm) the longest diameter of the target lesion in the axial, coronal, and sagittal planes, with the longest of these 3 measurements chosen as the final tumour size. Response was reported in the descriptive analysis as rCR, radiologic partial response (rPR), radiologic progressive disease (rPD), or radiologic stable disease (rSD), per the Response Evaluation Criteria in Solid Tumours (RECIST) 1.1 guideline. Radiologic complete response was defined as no residual enhancement on post-NAC MRI.

### *Pathological evaluation*

All pretreatment biopsies were reviewed by the pathology department at GUH. Pathology specimens were evaluated for hormone and human epidermal growth factor receptor expression via immunohistochemical testing, with confirmatory fluorescence in situ hybridisation (FISH) analysis, if indicated. This allowed the categorisation of the breast carcinomas into 1 of 4 biologic subtypes: Luminal A (oestrogen receptor [ER]/progesterone receptor [PR] positive, HER2 negative, Ki67 <20%), Luminal B (ER/PR positive, HER2 positive, or HER2 negative with Ki67 >20%), HER2/neu (ER/PR negative, HER2 positive), and triple negative (ER/PR/HER2 negative). Response to NAC and residual tumour size was assessed using postoperative pathology of the resected breast specimen by a consultant histopathologist at GUH. Pathologic complete response was defined as the absence of any invasive tumour in the examined specimen; however, the absence of in situ disease was excluded from this definition (pCR=ypT0/is).<sup>16</sup>

### *Statistical analysis*

Statistical analyses were performed using SPSS for Mac, version 26.0 (SPSS Inc, Armonk, NY, USA). Descriptive analysis was performed on included participants, with continuous variables being expressed as mean value, median, standard deviation (SD), minimum, and maximum; and categorical variables being expressed in percentage and 95% confidence interval (CI). Discrepancy between the measured tumour size on MRI and pathology specimen was evaluated and expressed in size (mm) ±SD. A Kolmogorov–Smirnov test was performed to evaluate normality of the quantitative discrepancy variables. The effect of different variables on MRI/pathology discrepancy was evaluated using the nonparametric Mann–Whitney test, for 2 groups, with the Kruskal–Wallis test used to compare data from 3 or more groups. Statistical significance level was set at 5%. Variables displaying statistical significance at univariate analysis were included as predictors in a binary logistic regression multivariate analysis. The efficacy of MRI in predicting pCR in sensitivity, specificity, positive predictive value

(PPV), negative predictive value (NPV), and accuracy was calculated. True-positive cases were defined as resulting in both rCR and pCR; false-positive cases had rCR without pCR; false-negative cases did not achieve rCR, but had pCR; and true-negative cases were negative for both rCR and pCR. These variables were calculated for each molecular breast cancer subtype (Luminal A, Luminal B, HER2/neu, and triple negative), as well as the rate of pCR (%). Chi-square testing was used to compare PPV and false-positivity rate between molecular subtypes. The Pearson correlation and the Spearman rank correlation were used, as appropriate, to compare MRI-measured and pathological tumour sizes, including subgroup analysis by molecular subtype.

### Endpoints

Positive and NPVs of MRI in predicting pCR and no pCR, respectively, were used as co-primary endpoints of the study. Our secondary endpoint was an analysis of factors influencing MRI accuracy in predicting final pathological tumour size.

### Results

Eighty-seven patients were included in this study. Mean age was 48.7 (21.0–73.0) years (Table 1). The mean (SD) tumour sizes on MRI at baseline and post-NAC were 43.6 mm (16.3 mm) and 18.8 mm (16.4 mm), respectively, with a final mean (SD) tumour size on pathology of 34.1 mm (31.9 mm). The median number of days between post-NAC MRI and surgery was 31.0 (range=4.0–134.0). The majority tumours were of Luminal A molecular subtype (58.6%, 51/87), with Luminal B and triple-negative subtypes being equally common (16.1%, 14/87) and HER2/neu subtype least common (9.2%, 8/82). The overall pCR rate was 19.5% (17/87), and the rCR rate was 28.7% (25/87). Human epidermal growth factor 2/neu subtype carcinomas displayed the highest rate of pCR (62.5%, 5/8), followed by triple-negative (28.6%, 4/14), Luminal B (21.4%, 3/14), and Luminal A (9.8%, 5/51) subtypes. Human epidermal growth factor 2/neu and triple-negative subtypes had equivalent rates of rCR (50.0%; HER2/neu 4/8, triple negative 7/14), followed by Luminal A (23.5%, 12/51) and Luminal B (14.3%, 2/14).

### MRI as a predictor of pCR

The PPV of MRI in predicting pCR was 36.0% (95% CI: [23.2%, 51.1%]) overall, whereas the NPV was 87.1% (95% CI: [80.1%, 91.9%]). The sensitivity, specificity, and accuracy of MRI in predicting pCR were 52.9% (95% CI: [27.8%, 77.0%]), 77.1% (95% CI: [65.6%, 86.3%]), and 72.4% (95% CI: [61.8%, 81.5%]), respectively. The diagnostic performance of MRI varied by molecular subtype (Table 2). The PPV was significantly lower in the Luminal A subtype (25.0%, 95% CI: [11.7%, 45.7%]) than in the Luminal B (50.0%, 95% CI: [7.9%, 92.1%]), HER2/neu (50.0%, 95% CI: [20.8%, 79.2%]), and triple-negative (42.9%, 95% CI: [22.5%, 65.9%]) subtypes.

PPV was significantly higher in nonluminal versus Luminal A disease (45.0% vs 25.0%,  $P < .001$ ), but this difference was not significant when Luminal B disease was included alongside Luminal A ( $P = .089$ ). The NPV was the highest in the Luminal A subtype (94.9%, 95% CI: [86.2%, 98.2%]), with lower rates in both Luminal B (83.3%, 95% CI: [68.7%, 91.9%]) and triple-negative (85.7%, 95% CI: [50.5%, 97.2%]) subtypes. However, the NPV was much lower for the HER2/neu (25.0%, 95% CI: [5.5%, 65.8%]) subtype. The overall false-positivity rate (rCR but no pCR) was 18.4% (16/87). False positivity also varied by molecular subtype, with the highest rate amongst the triple-negative subtype (28.6%, 4/14), followed by HER2/neu (25.0%, 2/8), Luminal A (17.6%, 9/51), and Luminal B (7.1%, 1/14). The higher rates of false positivity in nonluminal versus luminal subtypes reached statistical significance ( $P = .002$ ).

### MRI as a predictor of tumour size post-NAC

Eighty-three post-NAC MRI scans were evaluable for tumour size. Four scans were excluded due to the presence of small, multifocal lesions not amenable to measurement as a single maximum diameter. Among those excluded was 1 outlier who waited more than 100 days between preoperative MRI and surgery. The mean (SD) discrepancy between post-NAC MRI and final invasive pathological tumour size was 19.3 mm (24.2 mm), with a median of 11 mm, a minimum of 0.0 mm, and maximum of 115.0 mm. There was a statistically significant positive correlation overall between final tumour size on MRI and pathology (the Spearman  $\rho = 0.342$ ,  $P = .019$ , Figure 1). This mild/moderate statistically significant forward correlation was also observed in Luminal A (the Spearman  $\rho = 0.407$ ,  $P = .005$ , Figure 2) subtype, but failed to reach statistical significance in Luminal B (the Pearson correlation coefficient = .497,  $P = .071$ , Figure 2), HER2/neu (the Spearman  $\rho = -0.180$ ,  $P = .669$ , Figure 2), or triple-negative (the Spearman  $\rho = 0.317$ ,  $P = .269$ , Figure 2) subtypes. All tumours with a size discrepancy of greater than 50 mm between MRI and pathology were excluded ( $n = 5$ ), which increased the overall correlation markedly (the Spearman  $\rho = 0.615$ ,  $P < .001$ ).

### Factors influencing MRI accuracy in predicting post-NAC tumour size

Tumour grade had a significant impact on mean discrepancy between MRI and pathology ( $P = .001$ ), with higher grades of tumour displaying much lower mean discrepancy (Table 3). T category was also significantly associated with MRI accuracy, with lower mean discrepancy associated with cT1–2 category tumours. Infiltrating ductal carcinoma (IDC) had a significantly lower mean discrepancy in comparison to infiltrating lobular carcinoma (ILC) and luminal lesions displayed a higher mean discrepancy (ie, were less accurate) than nonluminal. Age, nodal status, and HER2 receptor status had no significant impact on mean discrepancy.

**Table 1.** Patient and tumour characteristics.

CONTINUOUS VARIABLES	MEAN	SD	MEDIAN	RANGE
Age (y)	48.7	10.3	49.0	21.0-73.0
Baseline tumour size on MRI (mm)	43.6	16.3	40.0	10.0-87.0
Post-NAC tumour size on MRI (mm)	18.8	16.4	18.0	0.0-68.0
Tumour size on pathology (mm)	34.1	31.9	28.0	0.0-140.0
Time to surgery after post-NAC MRI (days)	35.6	25.9	31.0	4.0-134.0
CATEGORICAL VARIABLES	SUBCATEGORY	N	% (95% CI)	
Surgical procedure	Mastectomy	39	44.8 [34.2, 55.9]	
	BCS	48	55.2 [44.1, 65.9]	
Nodal procedure	Axillary clearance	60	69.0 [58.1, 78.5]	
	SLN biopsy	27	31.0 [21.6, 41.9]	
Baseline tumour size (cT)	cT1	5	5.8 [1.9, 12.9]	
	cT2	55	63.2 [52.2, 73.3]	
	cT3	26	29.9 [20.5, 40.7]	
	cT4	1	1.1 [0.0, 6.2]	
Baseline nodal status (cN)	cN0	19	21.8 [13.7, 32.0]	
	cN1	52	59.8 [48.7, 70.2]	
	cN2	7	8.1 [3.3, 15.9]	
	cNx	9	10.3 [4.8, 18.7]	
Tumour size post-NAC (ypT)	ypT0	17	19.5 [11.8, 29.4]	
	ypT1	19	21.8 [13.7, 32.0]	
	ypT2	31	35.7 [25.7, 46.6]	
	ypT3	19	21.8 [13.7, 32.0]	
	ypT4	1	1.2 [0.0, 6.2]	
Nodal status post-NAC (ypN)	ypN0	40	46.0 [35.2, 57.0]	
	ypN1	25	28.7 [19.5, 39.4]	
	ypN2	14	16.1 [9.1, 25.5]	
	ypN3	8	9.2 [4.1, 17.3]	
Hormone receptor status	Positive	65	74.7 [64.3, 83.4]	
	Negative	22	25.3 [16.6, 35.8]	
Molecular subtype	Luminal A	51	58.6 [47.6, 69.1]	
	Luminal B	14	16.1 [9.1, 25.5]	
	HER2/neu	8	9.2 [4.1, 17.3]	
	Triple negative	14	16.1 [9.1, 25.5]	
Histological subtype	Ductal	70	80.5 [70.6, 88.2]	
	Lobular	13	14.9 [8.2, 24.2]	
	Other <sup>a</sup>	4	4.6 [1.3, 11.4]	

(Continued)

**Table 1.** (Continued)

CONTINUOUS VARIABLES	MEAN	SD	MEDIAN	RANGE
Histological grade	G1		3	3.5 [0.7, 9.8]
	G2		46	52.9 [41.9, 63.7]
	G3		38	43.7 [33.1, 54.7]
	NA		2	2.3 [0.3, 8.1]
Radiologic response	rCR		25	28.7 [19.5, 39.4]
	rPR		46	52.9 [41.9, 63.7]
	rPD		0	0.0 <sup>b</sup> [0.0, 4.1]
	rSD		16	18.4 [10.9, 28.1]
Pathological response	pCR		17	19.5 [11.8, 29.4]
	No pCR		70	80.5 [70.6, 88.2]
Adjuvant therapy	Radiotherapy		78	94.0 <sup>c</sup> [86.5, 98.0]
	Endocrine		64	73.6 <sup>d</sup> [63.0, 82.5]
	Trastuzumab		21	24.1 <sup>e</sup> [15.6, 34.5]

Abbreviations: BCS, breast-conserving surgery; CI, confidence interval; HER2, human epidermal growth factor 2; MRI, magnetic resonance imaging; NA, not available; NAC, neoadjuvant chemotherapy; pCR, pathologic complete response; rCR, radiologic complete response; rPD, radiologic progressive disease; rPR, radiologic partial response; rSD, radiologic stable disease; SD, standard deviation; SLN, sentinel lymph node.

<sup>a</sup>Other subtypes included 1× spindle cell, 2× mucinous, and 1× metaplastic.

<sup>b</sup>One-sided 97.5% CI.

<sup>c</sup>94.0 valid percent (78/83 included patients, data missing on 4 patients).

<sup>d</sup>100.0% (95% CI: [94.5%, 100.0%], n=65/65) of hormone receptor-positive patients received endocrine therapy.

<sup>e</sup>95.5% (95% CI: [77.2%, 99.9%], n=21/22) HER2 receptor-positive patients received trastuzumab.

**Table 2.** MRI diagnostic performance in predicting pathologic complete response for various molecular subtypes, % (95% confidence interval).

	OVERALL (N=87)	LUMINAL A (N=51)	LUMINAL B (N=14)	HER2/NEU (N=8)	TRIPLE NEGATIVE (N=14)
Sensitivity	52.9% [27.8%, 77.0%]	60.0% [14.6%, 94.7%]	33.3% [0.8%, 90.6%]	40.0% [5.2%, 85.3%]	75.0% [19.4%, 99.4%]
Specificity	77.1% [65.6%, 86.3%]	80.5% [66.1%, 90.6%]	90.9% [58.7%, 99.8%]	33.3% [0.8%, 90.6%]	60.0% [26.2%, 88.8%]
PPV	36.0% [23.2%, 51.1%]	25.0% [11.7%, 45.7%]	50.0% [7.9%, 92.1%]	50.0% [20.8%, 79.2%]	42.9% [22.5%, 65.9%]
NPV	87.1% [80.1%, 91.9%]	94.9% [86.2%, 98.2%]	83.3% [68.7%, 91.9%]	25.0% [5.5%, 65.8%]	85.7% [50.5%, 97.2%]
Accuracy	72.4% [61.8%, 81.5%]	78.4% [64.7%, 88.7%]	78.6% [49.2%, 95.3%]	37.5% [8.5%, 75.5%]	64.3% [35.1%, 87.2%]

Abbreviations: HER2, human epidermal growth factor 2; MRI, magnetic resonance imaging; NPV, negative predictive value; PPV, positive predictive value.

Triple-negative subtype had the lowest mean (SD) discrepancy of 7.6 mm (10.3 mm), followed by HER2/neu 9.6 mm (12.9 mm), Luminal B 15.6 mm (11.1 mm), and Luminal A 25.5 mm (29.2 mm). Although the *P* value for molecular subtype appears to be statistically significant (*P* = .027), when adjusted for multiple comparisons by the Bonferroni method, no 2 group comparators reached statistical significance. Triple-negative and Luminal A subtypes displayed the most visually notable difference (Figure 3), but this failed to reach adjusted statistical significance (*P* = .057). After multivariate linear regression analysis, tumour grade (*P* = .036), cT (*P* < .001), and histological subtype (*P* = .04) remained significant independent predictors of MRI accuracy of mean discrepancy (Table 4). Among the variables which reached statistical significance on

multivariate analysis, MRI tended to overestimate the tumour size in high grade (48.6%), low cT (56.9%), and ductal (55.2%) type tumours (Appendix 1).

## Discussion

Neoadjuvant chemotherapy has resulted in increased rates of breast-conserving surgery (BCS), due to its ability to reduce the size and extent of the primary tumour.<sup>17</sup> Neoadjuvant chemotherapy can also result in a pCR or a complete tumour remission. The ability to predict pCR post-NAC accurately and consistently is important. Pathologic complete response can be used as an endpoint for clinical efficacy and regulatory approval of neoadjuvant agents in cancer trials, and accurate noninvasive imaging could accelerate this process for the



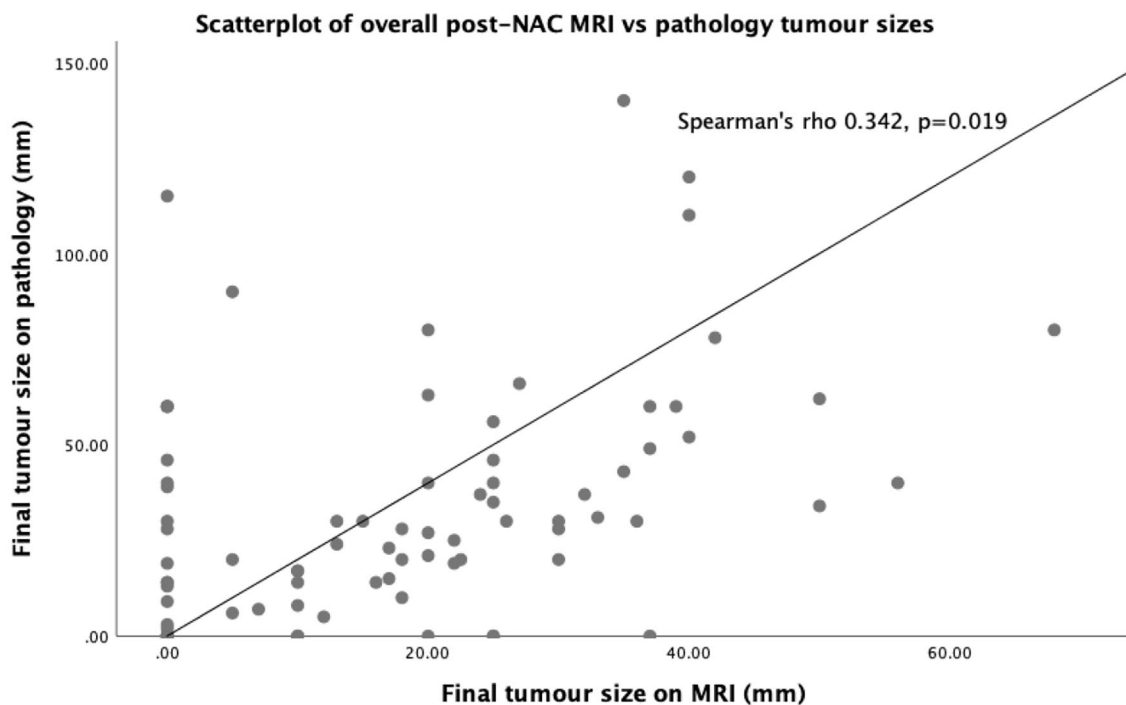


**Figure 1.** MRI indicates magnetic resonance imaging; NAC, neoadjuvant chemotherapy.

benefit of patients.<sup>18</sup> Accurate estimation of the residual tumour size and location is also vital for surgical planning to ensure that the minimum amount of tissue is removed while achieving an oncologic resection.

Magnetic resonance imaging has shown superiority to other modalities regarding pCR prediction; however, the diagnostic accuracy of MRI is highly variable in the literature.<sup>9,19-21</sup> This study found that MRI could predict pCR with a sensitivity, specificity, PPV, and NPV of 52.9%, 77.1%, 36.0%, and 87.1%, respectively, with an overall accuracy of 72.4%. This pattern of high NPV and specificity, with a lower sensitivity and PPV is mirrored in a systematic review by Lobbes et al,<sup>21</sup> who report a median sensitivity, specificity, PPV, and NPV of 42%, 89%, 64%, and 87%, respectively. More recent work by Kaise et al and Bouzón et al had similar findings, although they defined MRI accuracy regarding ability to detect residual tumour, rather than to predict pCR, so the PPV is equivalent to the definition of NPV in this study, and sensitivity and specificity are similarly swapped.<sup>13,22,23</sup> The PPV was significantly higher for nonluminal versus Luminal A disease, but this significance did not persist when Luminal B disease was analysed alongside Luminal A. The Luminal B disease cohort were all hormone receptor (HR) and HER2 positive in our cohort, which may have influenced this outcome. Murphy et al<sup>24</sup> found MRI accuracy to be much higher in HER2-positive breast cancer. Our small HER2/neu sample size ( $n=8$ ) limits our ability to comment definitively on this subtype. However, the HER2/neu breast cancers were overall least accurate in our cohort and Luminal B cancers were most accurate, making it difficult to delineate any clear directional

association between HER2 positivity and MRI accuracy. The rate of pCR was the highest in the HER2/neu subtype, likely due to the use of HER2-targeted agents used in the neoadjuvant setting.<sup>23</sup> Although rCR on MRI therefore shows a reasonable and consistent ability to predict pCR, the high false-positive rate (rCR but no pCR) of 18% in this study makes the prospect of avoiding surgery based on MRI findings untenable. There is an appetite amongst health care professionals to pursue avenues of surgery avoidance in select patients, however.<sup>25</sup> Currently, under investigation is the selective use of post-NAC biopsies of the residual tumour bed, using either ultrasound or MRI guidance, in trials such as MICRA,<sup>26</sup> RESPONDER,<sup>27</sup> NOSTRA,<sup>28</sup> NCT02945579,<sup>29</sup> and CRBr,<sup>30</sup> among others. Early results show promise in the MRI-guided biopsy group,<sup>5,29</sup> with mixed results for the ultrasound-guided cohort.<sup>26,28</sup>

The correlation between final tumour size on MRI and on pathology in this study was relatively weak ( $\rho=0.342$ ,  $P=.019$ ). In a review of 17 studies, Lobbes et al<sup>21</sup> reported a median correlation coefficient of 0.698 (range=0.21-0.982), with only 2 studies failing to achieve statistical significance in their correlation analysis. Chen et al<sup>31</sup> observed a marked increase in correlation coefficient when lesions with size discrepancy greater than 5 cm were excluded from the analysis, and this was also observed in our cohort. The small sample sizes within all but the Luminal A subtype in this study limited the utility of delineating correlation coefficients by molecular subtype. The relationship between final MRI and pathology tumour sizes was further evaluated through mean discrepancy. The lowest mean discrepancy was seen in the

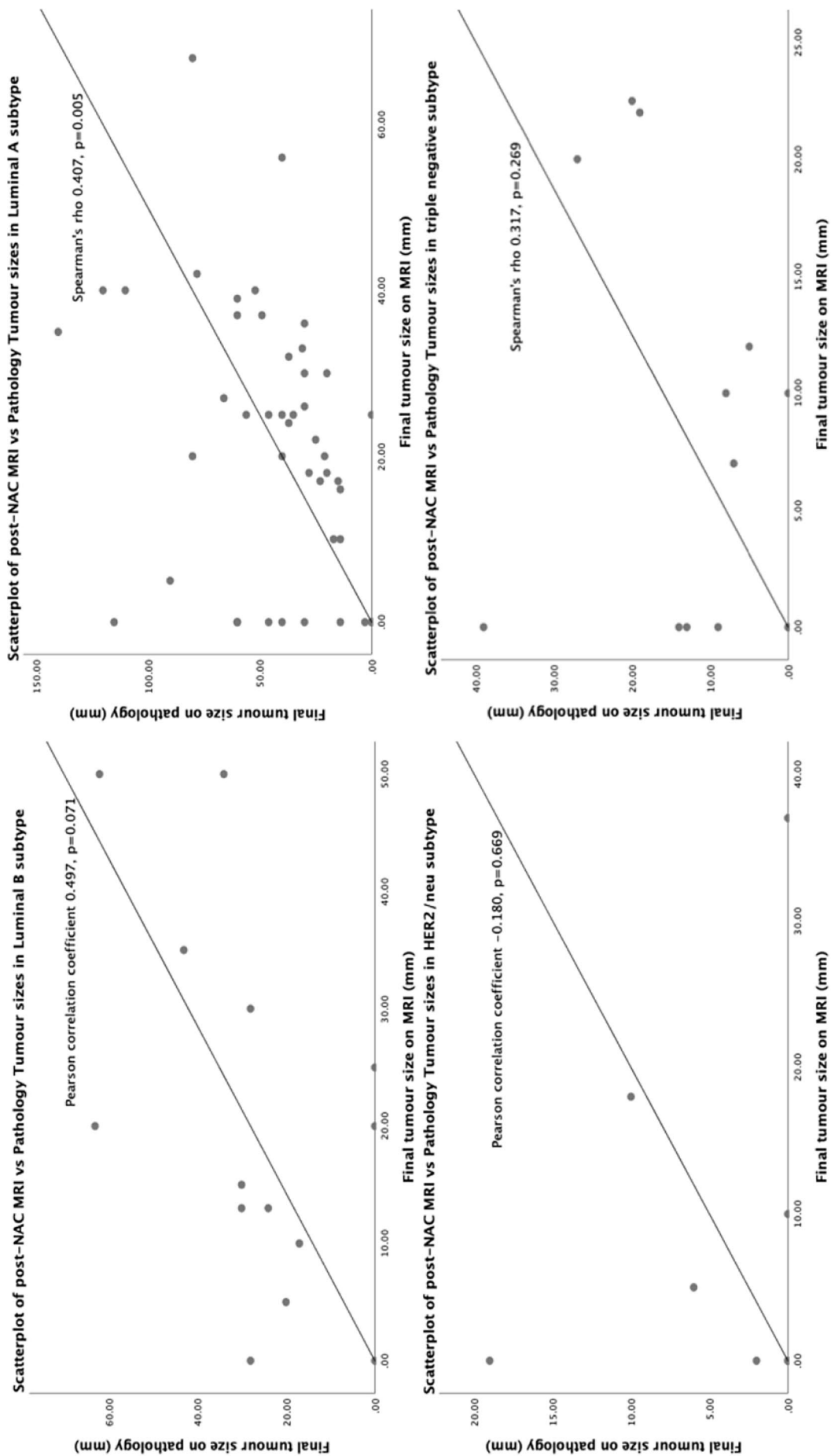


Figure 2. HER2 indicates human epidermal growth factor 2; MRI, magnetic resonance imaging; NAC, neoadjuvant chemotherapy.

**Table 3.** Univariate analysis of factors influencing MRI accuracy of mean discrepancy between post-NAC MRI and pathologic tumour sizes.

VARIABLE	N	MEAN DISCREPANCY ( $\pm$ SD)	P VALUE
Age (y)			
>45	49	20.2 mm ( $\pm$ 23.1 mm)	.244
$\leq$ 45	34	17.9 mm ( $\pm$ 26.0 mm)	
cN			
0	19	15.4 mm ( $\pm$ 24.2 mm)	.425
1+	64	21.7 mm ( $\pm$ 25.4 mm)	
Grade			
1-2	48	26.6 mm ( $\pm$ 28.8 mm)	<b>.002</b>
3	35	9.6 mm ( $\pm$ 11.2 mm)	
cT			
1-2	59	11.8 mm ( $\pm$ 13.8 mm)	<b>&lt;.001</b>
3+	24	37.8 mm ( $\pm$ 33.3 mm)	
Histological subtype*			
Ductal	67	15.4 mm ( $\pm$ 19.8 mm)	<b>.001</b>
Lobular	12	41.8 mm ( $\pm$ 35.8 mm)	
HR status			
Positive	61	23.2 mm ( $\pm$ 26.4 mm)	<b>.002</b>
Negative	22	8.3 mm ( $\pm$ 11.0 mm)	
HER2			
Positive	22	13.5 mm ( $\pm$ 11.9 mm)	.733
Negative	61	21.4 mm ( $\pm$ 27.1 mm)	
Molecular subtype			
Luminal A	47	25.5 mm ( $\pm$ 29.2 mm)	.027**
Luminal B	14	15.6 mm ( $\pm$ 11.1 mm)	
HER2/neu	8	9.6 mm ( $\pm$ 12.9 mm)	
Triple negative	14	7.6 mm ( $\pm$ 10.3 mm)	

Abbreviations: cN, clinical nodal status; cT, clinical tumour stage; HER2, human epidermal growth factor 2; HR, hormone receptor; MRI, magnetic resonance imaging; NAC, neoadjuvant chemotherapy; SD, standard deviation.

Numbers in bold denote factors which reached statistical significance.

\*1 $\times$  spindle cell, 2 $\times$  mucinous, and 1 $\times$  metaplastic subtypes excluded for this analysis.

\*\*P value nonsignificant when adjusted for multiple comparisons by the Bonferroni method.

triple-negative subtype. This increased accuracy in triple-negative breast cancer may be related to its concentric regression pattern post-NAC.<sup>32</sup> Factors that independently and significantly impacted MRI accuracy were tumour grade, size, and histological subtype. Tumours of higher grade and lower cT showed lower mean discrepancies, which is a consistent finding in the literature.<sup>23,33</sup> Tumours of higher grade and lower cT have also been shown to have a better response to chemotherapy, and MRI is reportedly more accurate in chemoresponsive breast cancers, which may explain the observed lower mean discrepancy in these groups.<sup>23</sup> Magnetic resonance imaging tended to overestimate the tumour size in high grade, low cT, and ductal type tumours. Magnetic resonance imaging underestimated tumour size in the vast majority of Lobular breast cancers (91.7%). Lobular breast cancers represent a more heterogeneous group than ductal carcinomas, some of which may be less responsive to NAC, and this might explain the inaccuracy observed in this cohort.<sup>34</sup>

Evaluation of tumour diameter on MRI alone is therefore clearly insufficient to accurately predict pCR and final tumour size, although this accuracy improves with increasing tumour grade, decreasing tumour size, and ductal type tumours. Some other strategies which have been employed to increase the diagnostic accuracy of MRI images include volumetric<sup>35,36</sup> and radiomic<sup>37</sup> analysis, machine learning algorithms,<sup>38</sup> and different MRI protocols, including diffusion weighted imaging.<sup>39</sup>

The strength of this study lies in the robust consideration of patient and tumour characteristics contributing to MRI accuracy. Nonetheless, there are a number of limitations to this study. This is a single-centre retrospective study, and contains only a small number of nonluminal subtype breast cancers (HER2/neu [n=8] and triple negative [n=14]). This likely resulted in a high risk of Type 2 error, and there was no significant difference between mean discrepancy of triple-negative and luminal breast cancer ( $P=.056$ ), despite strong evidence for this in previous publications.<sup>22</sup> This study did not evaluate the impact of nonmass-like enhancing lesions on MRI accuracy, and the MRI machine used had a 1.5-T magnet, as opposed to the higher resolution 3T magnet; both of which have been shown to be of significance.<sup>40</sup>

In conclusion, preoperative, post-NAC MRI does not accurately predict tumour response to NAC across all breast cancer subtypes. For pCR prediction, nonluminal disease is superior to luminal A of PPV. Tumour size, grade, and histological subtype should be taken into consideration when evaluating the preoperative MRIs for BCS planning in these patients. Further research could focus on adjunctive strategies, such as radiomic and machine learning models, to help improve MRI performance and utility in predictive response to NAC.



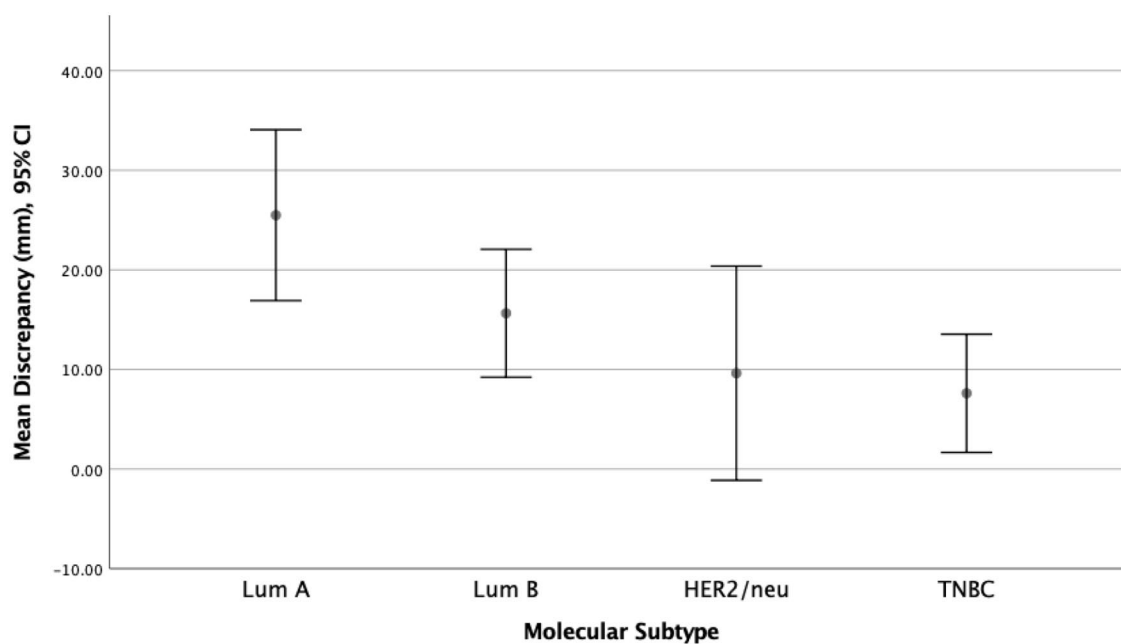


**Figure 3.** Discrepancy between post-NAC tumour size as measured on MRI versus pathologic specimen based on molecular subtype (mm): (mean  $\pm$  SD), Luminal A ( $25.5 \pm 29.2$ ), Luminal B ( $15.6 \pm 11.1$ ), HER2/neu ( $9.6 \pm 12.9$ ), and triple negative ( $7.6 \pm 10.3$ ). CI indicates confidence interval; HER2, human epidermal growth factor 2; MRI, magnetic resonance imaging; NAC, neoadjuvant chemotherapy.

**Table 4.** Multivariate regression analysis.

ADJUSTED $R^2=0.387$				
INDEPENDENT VARIABLES	B	SE	P VALUE	95% CI
Grade	-10.787	5.041	<b>.036</b>	[-20.837, -0.738]
cT	11.816	2.477	<b>&lt;.001</b>	[6.879, 16.753]
Histological subtype	18.689	6.363	<b>.004</b>	[6.005, 31.373]
HR status	3.855	5.774	.506	[-7.665, 15.365]

Abbreviations: B, unstandardised coefficients; CI, confidence interval; cT, T category; HR, hormone receptor; SE, standard error. Numbers in bold denote factors which reached statistical significance.

## Appendix 1

Tendency of MRI towards overestimation or underestimation of final tumour size versus pathology.

VARIABLE	N	OVERESTIMATED	UNDERESTIMATED	DIFFERENCE $\leq 1$ MM
Age (y)				
>45	49	22.4%	63.3%	14.3%
$\leq 45$	34	23.5%	58.8%	17.7%
cN				
0	19	42.1%	52.6%	5.3%
1+	64	20.0%	61.8%	18.2%

(Continued)

## Appendix 1. (Continued)

VARIABLE	N	OVERESTIMATED	UNDERESTIMATED	DIFFERENCE $\leq 1$ MM
Grade <sup>a</sup>				
1-2	48	16.7%	70.8%	12.5%
3	35	31.4%	48.6%	20.0%
cT <sup>a</sup>				
1-2	58	20.7%	56.9%	22.4%
3+	25	28.0%	72.0%	0.0%
Histological subtype <sup>a</sup>				
Ductal	67	25.4%	55.2%	19.4%
Lobular	12	91.7%	8.3%	0.0%
HR status				
Positive	61	18.0%	72.1%	9.9%
Negative	22	36.4%	31.8%	31.8%
HER2				
Positive	22	31.8%	50.0%	18.2%
Negative	61	19.7%	14.7%	65.6%
Molecular subtype				
Luminal A	47	14.9%	74.5%	10.6%
Luminal B	14	28.6%	64.3%	7.1%
HER2/neu	8	37.5%	37.5%	25.0%
Triple negative	14	35.7%	35.7%	28.6%

Abbreviations: cN, clinical nodal status; cT, clinical tumour stage; HER2, human epidermal growth factor 2; HR, hormone receptor; MRI, magnetic resonance imaging.

<sup>a</sup>Variables that reached statistical significance after multivariate regression analysis.

## Author Contributions

RB study conception, data extraction, article planning, drafting, coordination, and revision; PMcA article planning, revision; NOH data collation and extraction; BM article planning and revision; EC data collation and extraction, article revision; MK article planning, article revision, primary surgeon for many of the included patients, AL article planning, article revision, primary surgeon for many of the included patients. All authors read and approved the final article.

## Data Availability

The data sets generated during and/or analysed during this study are available from the corresponding author on reasonable request.

## ORCID iD

Robert Browne  <https://orcid.org/0000-0003-4092-2328>

## REFERENCES

1. Henley SJ, Ward EM, Scott S, et al. Annual report to the nation on the status of cancer, part I: national cancer statistics. *Cancer*. 2020;126:2225-2249.
2. Thomssen C, Balic M, Harbeck N, Gnant M. St. Gallen/Vienna 2021: a brief summary of the consensus discussion on customizing therapies for women with early breast cancer. *Breast Care (Basel)*. 2021;16:135-143.
3. Long-term outcomes for neoadjuvant versus adjuvant chemotherapy in early breast cancer: meta-analysis of individual patient data from ten randomised trials. *Lancet Oncol*. 2018;19:27-39.
4. Boughey JC, McCall LM, Ballman KV, et al. Tumor biology correlates with rates of breast-conserving surgery and pathologic complete response after neoadjuvant chemotherapy for breast cancer: findings from the ACOSOG Z1071 (Alliance) Prospective Multicenter Clinical Trial. *Ann Surg*. 2014;260:608-614; discussion 614-616.
5. Sutton EJ, Braunstein LZ, El-Tamer MB, et al. Accuracy of magnetic resonance imaging-guided biopsy to verify breast cancer pathologic complete response after neoadjuvant chemotherapy: a nonrandomized controlled trial. *JAMA Netw Open*. 2021;4:e2034045.
6. Heil J, Kuerer HM, Pfof A, et al. Eliminating the breast cancer surgery paradigm after neoadjuvant systemic therapy: current evidence and future challenges. *Ann Oncol*. 2020;31:61-71.
7. Kong X, Moran MS, Zhang N, Haffty B, Yang Q. Meta-analysis confirms achieving pathological complete response after neoadjuvant chemotherapy predicts favourable prognosis for breast cancer patients. *Eur J Cancer*. 2011;47:2084-2090.

8. Cortazar P, Zhang L, Untch M, et al. Pathological complete response and long-term clinical benefit in breast cancer: the CTNeoBC pooled analysis. *Lancet*. 2014;384:164-172.
9. Chagpar AB, Middleton LP, Sahin AA, et al. Accuracy of physical examination, ultrasonography, and mammography in predicting residual pathologic tumor size in patients treated with neoadjuvant chemotherapy. *Ann Surg*. 2006;243:257-264.
10. Jarrett AM, Hormuth DA, Adhikarla V, et al. Towards integration of 64Cu-DOTA-trastuzumab PET-CT and MRI with mathematical modeling to predict response to neoadjuvant therapy in HER2 + breast cancer. *Sci Rep*. 2020;10:20518.
11. Tokuda Y, Yanagawa M, Fujita Y, et al. Prediction of pathological complete response after neoadjuvant chemotherapy in breast cancer: comparison of diagnostic performances of dedicated breast PET, whole-body PET, and dynamic contrast-enhanced MRI. *Breast Cancer Res Treat*. 2017;188:107-115.
12. Reig B, Heacock L, Lewin A, Cho N, Moy L. Role of MRI to assess response to neoadjuvant therapy for breast cancer. *J Magn Reson Imaging*. 2020;52:12.
13. Kaise H, Shimizu F, Akazawa K, et al. Prediction of pathological response to neoadjuvant chemotherapy in breast cancer patients by imaging. *J Surg Res*. 2018;225:175-180.
14. Zhang X, Wang D, Liu Z, et al. The diagnostic accuracy of magnetic resonance imaging in predicting pathologic complete response after neoadjuvant chemotherapy in patients with different molecular subtypes of breast cancer. *Quant Imaging Med Surg*. 2020;10:197-210.
15. Mann RM, Cho N, Moy L. Breast MRI: state of the Art. *Radiology*. 2019;292:520-536.
16. Santamaria G, Bargalló X, Ganau S, et al. Multiparametric MR imaging to assess response following neoadjuvant systemic treatment in various breast cancer subtypes: comparison between different definitions of pathologic complete response. *Eur J Radiol*. 2019;117:132-139.
17. Li X, Dai D, Chen B, Tang H, Wei W. Oncological outcome of complete response after neoadjuvant chemotherapy for breast conserving surgery: a systematic review and meta-analysis. *World J Surg Oncol*. 2017;15:210.
18. U.S. Department of Health and Human Services Food and Drug Administration OCoE, Center for Drug Evaluation and Research (CDER), Center for Biologics Evaluation and Research (CBER). *Pathological Complete Response in Neoadjuvant Treatment of High-Risk Early-Stage Breast Cancer: Use as an End-point to Support Accelerated Approval Guidance for Industry*. Silver Spring, MD: Food and Drug Administration; 2020. <https://www.fda.gov/media/83507/download>.
19. Yuan Y, Chen XS, Liu SY, Shen KW. Accuracy of MRI in prediction of pathologic complete remission in breast cancer after preoperative therapy: a meta-analysis. *Am J Roentgenol*. 2010;195:260-268.
20. Wu LM, Hu JN, Gu HY, Hua J, Chen J, Xu JR. Can diffusion-weighted MR imaging and contrast-enhanced MR imaging precisely evaluate and predict pathological response to neoadjuvant chemotherapy in patients with breast cancer? *Breast Cancer Res Treat*. 2012;135:17-28.
21. Lobbes MB, Prevors R, Smidt M, et al. The role of magnetic resonance imaging in assessing residual disease and pathologic complete response in breast cancer patients receiving neoadjuvant chemotherapy: a systematic review. *Insights Imaging*. 2013;4:163-175.
22. Bouzón A, Acea B, Soler R, et al. Diagnostic accuracy of MRI to evaluate tumour response and residual tumour size after neoadjuvant chemotherapy in breast cancer patients. *Radiol Oncol*. 2016;50:73-79.
23. Bouzón A, Iglesias Á, Acea B, Mosquera C, Santiago P, Mosquera J. Evaluation of MRI accuracy after primary systemic therapy in breast cancer patients considering tumor biology: optimizing the surgical planning. *Radiol Oncol*. 2019;53:171-177.
24. Murphy C, Mukaro V, Tobler R, et al. Evaluating the role of magnetic resonance imaging post-neoadjuvant therapy for breast cancer in the NEONAB trial. *Intern Med J*. 2018;48:699-705.
25. Gharzai LA, Szczygiel LA, Shumway DA, et al. A qualitative study to evaluate physician attitudes regarding omission of surgery among exceptional responders to neoadjuvant systemic therapy for breast cancer (NRG-CC006). *Breast Cancer Res Treat*. 2021;187:777-784.
26. van Loevezijn AA, van der Noorda MEM, van Werkhoven ED, et al. Minimally invasive complete response assessment of the breast after neoadjuvant systemic therapy for early breast cancer (MICRA trial): interim analysis of a multicenter observational cohort study. *Ann Surg Oncol*. 2021;28:3243-3253.
27. Heil J, Pfob A, Sinn H-PP, et al. Abstract GS5-03: diagnosing residual disease and pathologic complete response after neoadjuvant chemotherapy in breast cancer patients by image-guided vacuum-assisted breast biopsy: results of a prospective multicenter trial. *Cancer Res*. 2020;80:GS5-03.
28. Francis A, Herring K, Molyneux R, et al. NOSTRA PRELIM: a non randomised pilot study designed to assess the ability of image guided core biopsies to detect residual disease in patients with early breast cancer who have received neoadjuvant chemotherapy to inform the design of a planned trial [abstract]. Proceedings of the 2016 San Antonio Breast Cancer Symposium; 2016 Dec 6-10; San Antonio, TX. Philadelphia (PA): AACR. *Cancer Res*. 2017;77:Abstract P5-16-14.
29. Kuerer HM, Rauch GM, Krishnamurthy S, et al. A clinical feasibility trial for identification of exceptional responders in whom breast cancer surgery can be eliminated following neoadjuvant systemic therapy. *Ann Surg*. 2018;267:946-951.
30. Hariharan N, Rao TS, Rajappa S, et al. Accuracy of core biopsy in predicting pathologic complete response in the breast in patients with complete/near complete clinical and radiological response (Complete Responders in the Breast – CRBr) – trial design and conduct. *Int J Surg Protoc*. 2019;16:5-8.
31. Chen J-H, Bahri S, Mehta RS, et al. Breast cancer: evaluation of response to neoadjuvant chemotherapy with 3.0-T MR imaging. *Radiology*. 2011;261:735-743.
32. Eom HJ, Cha JH, Choi WJ, Chae EY, Shin HJ, Kim HH. Predictive clinico-pathologic and dynamic contrast-enhanced MRI findings for tumor response to neoadjuvant chemotherapy in triple-negative breast cancer. *Am J Roentgenol*. 2017;208:W225-W230.
33. De Los Santos JF, Cantor A, Amos KD, et al. Magnetic resonance imaging as a predictor of pathologic response in patients treated with neoadjuvant systemic treatment for operable breast cancer. Translational Breast Cancer Research Consortium trial 017. *Cancer*. 2013;119:1776-1783.
34. Lips EH, Mukhtar RA, Yau C, et al. Lobular histology and response to neoadjuvant chemotherapy in invasive breast cancer. *Breast Cancer Res Treat*. 2012;136:35-43.
35. Musall BC, Abdelhafez AH, Adrada BE, et al. Functional tumor volume by fast dynamic contrast-enhanced MRI for predicting neoadjuvant systemic therapy response in triple-negative breast cancer. *J Magn Reson Imaging*. 2021;54:251-260.
36. Ding J, Xiao H, Deng W, Liu F, Zhu R, Ha R. Feasibility of quantitative and volumetric enhancement measurement to assess tumor response in patients with breast cancer after early neoadjuvant chemotherapy. *J Int Med Res*. 2021;49:300060521991017.
37. Zhou J, Lu J, Gao C, et al. Predicting the response to neoadjuvant chemotherapy for breast cancer: wavelet transforming radiomics in MRI. *BMC Cancer*. 2020;20:100.
38. Sutton EJ, Onishi N, Fehr DA, et al. A machine learning model that classifies breast cancer pathologic complete response on MRI post-neoadjuvant chemotherapy. *Breast Cancer Res*. 2020;22:57.
39. Suo S, Yin Y, Geng X, et al. Diffusion-weighted MRI for predicting pathologic response to neoadjuvant chemotherapy in breast cancer: evaluation with mono-, bi-, and stretched-exponential models. *J Transl Med*. 2021;19:236.
40. Chen JH, Bahri S, Mehta RS, et al. Impact of factors affecting the residual tumor size diagnosed by MRI following neoadjuvant chemotherapy in comparison to pathology. *J Surg Oncol*. 2014;109:158-167.